Time to reach near-steady state in large aquifers

P. Rousseau-Gueutin, A. J. Love, G. Vasseur, N. I. Robinson, C. T. Simmons, G. De Marsily

WATER RESOURCES RESEARCH, VOL. 49, 6893–6908, doi:10.1002/wrcr.20534, 2013

Time to reach near-steady state in large aquifers

P. Rousseau-Gueutin,[1,2] A. J. Love,[1,3] G. Vasseur,[4,5] N. I. Robinson,[1]
C. T. Simmons,[1,3] and G. de Marsily[4,5]

Received 17 May 2013; revised 9 September 2013; accepted 14 September 2013; published 23 October 2013.

[1] A new analytical solution of the flow equation has been developed to estimate the time to reach a near-equilibrium state in mixed aquifers, i.e., having unconfined and confined portions, following a large hydraulic perturbation. Near-equilibrium is defined as the time for an initial aquifer perturbation to dissipate by an average 95% across the aquifer. The new solution has been obtained by solving the flow system of a simplified conceptual model of a mixed aquifer using Laplace transforms. The conceptual model is based on two assumptions: (1) the groundwater flow can be reduced to a horizontal 1-D problem and (2) the transmissivity, a function of the saturated thickness, is assumed constant on the unconfined portion. This new solution depends on the storativity of the unconfined portion, the lengths of the unconfined and confined portions and the transmissivity, assumed to be constant and equal in both portions of the mixed aquifer. This solution was then tested and validated against a numerical flow model, where the variations of the saturated thickness and therefore variations of the transmissivity were either ignored, or properly modeled. The agreement between the results from the new solution and those from the numerical model is good, validating the use of this new solution to estimate the time to reach near-equilibrium in mixed aquifers. This solution for mixed aquifers, as well as the solutions for a fully confined or fully unconfined aquifer, has been used to estimate the time to reach near-equilibrium in 13 large aquifers in the world. For those different aquifers, the time to reach near-equilibrium ranges between 0.7 kyr to 2.4×10^7 kyr. These results suggest that the present hydraulic heads in these aquifers are typically a mixture of responses induced from current and past hydrologic conditions and thus climate conditions. For some aquifers, the modern hydraulic heads may in fact depend upon hydrologic conditions resulting from several past climate cycles.

Citation: Rousseau-Gueutin, P., A. J. Love, G. Vasseur, N. I. Robinson, C. T. Simmons, and G. de Marsily (2013), Time to reach near-steady state in large aquifers, *Water Resour. Res.*, *49*, 6893–6908, doi:10.1002/wrcr.20534.

1. Introduction

[2] Estimating the current hydrodynamic state of aquifers is crucial for modeling them accurately. One requires knowledge of whether an aquifer system is in steady state with respect to recharge and discharge or if it is in a transient state where recharge does not equal discharge.

[3] Changes in recharge, discharge, or hydraulic parameters can result in the groundwater system being in disequilibrium which will initiate some transient groundwater behavior. Different mechanisms such as geologic processes [*Luo*, 1994; *Neuzil*, 1995; *Gonçalvès et al*., 2004], or morphologic and climatic variations [*Love et al*., 1994; *Gonçalvès et al*., 2004; *Jost et al*., 2007] can lead to hydrodynamic changes. Transient behaviors of groundwater systems are related to a balance between the origin of the perturbation and the resulting flows, which tend to dissipate it. A major control of this dissipation is the aquifer diffusivity, the ratio of aquifer transmissivity to storativity.

[4] In aquitards with low permeability, long-term transient behavior can occur due to their low hydraulic diffusivity [*de Marsily*, 1986; *Neuzil*, 1995]. Conversely, in aquifers with higher hydraulic diffusivity, one would expect the transient behavior to occur over shorter time periods as they adjust more rapidly to any hydraulic perturbation [*Neuzil*, 1995]. However, several studies, based on numerical models, have examined the effect of past climatic conditions on present-day hydrodynamics [*Burdon*, 1977; *Lloyd and Farag*, 1978; *Dieng et al*., 1990; *Love et al*., 1994; *de Vries*, 1997; *Coudrain et al*., 2001; *Houston and Hart*, 2004; *Jost et al*., 2007; *Sy and Besbes*, 2008]

Additional supporting information may be found in the online version of this article.

[1]School of the Environment, Flinders University, Adelaide, South Australia, Australia.
[2]École des Hautes Études en Santé Publique, Avenue du Professeur Léon Bernard, Rennes, France.
[3]National Centre for Groundwater Research and Training, Flinders University, Adelaide, South Australia, Australia.
[4]Université Pierre et Marie Curie, Paris 6, UMR-7619 SISYPHE, Paris, France.
[5]CNRS, UMR-7619 SISYPHE, Paris, France.

Corresponding author: P. Rousseau-Gueutin, School of the Environment, Flinders University, GPO Box 2100, Adelaide, SA 5001, Australia. (pauline_gueutin@yahoo.fr)

0043-1397/13/10.1002/wrcr.20534

showing that aquifers may present long-term transient behaviors due to past-climatic variations.

[5] Transient behavior, such as occurs after any sudden change of hydraulic conditions, results in a nearly exponential relaxation toward a new steady state. This exponential relaxation is characterized by a time constant τ, which is a function of the storativity, transmissivity, and length of the aquifer, as will be shown later, or as shown by *Domenico and Schwartz* [1998]. After a hydraulic perturbation, such as the cessation of recharge, the time to reach a near-steady state or near-equilibrium (t_{NE}) can be estimated from the knowledge of τ. The knowledge of t_{NE} is important to assess the hydrodynamic state of aquifers, i.e., steady state versus transient, and therefore to model them appropriately. Solution formulae exist to estimate the time constant for fully confined [*Domenico and Schwartz*, 1998] or fully unconfined aquifers [*Reilly and Harbaugh*, 2004]. We are unaware of any solution formula that has been proposed to estimate this time constant in mixed aquifers, i.e., hydrogeologic systems which are partly unconfined and partly confined. Although, the estimation of t_{NE} is crucial to assess the hydrodynamic state of aquifers, only a few studies have applied this methodology [*York et al*., 2002; *Schwartz et al*., 2009]. These previous studies have examined small-size to medium-size aquifers (40–70 km) in length. This study focuses on the estimation of t_{NE} for large mixed aquifers, i.e., with a size of several hundreds of kilometers.

[6] The purpose of this work is to develop and test a new time constant, τ_m, for mixed aquifers in order to assess their hydrodynamic state as a simple first approximation avoiding the use of numerical models, which could be time consuming. This new solution has been obtained using a Laplace transform analysis of the equation describing flow in a conceptual model of an unconfined-confined aquifer submitted to an initial disequilibrium with a long-term disturbance. This new formulation has been tested by comparison with a numerical model whose geometry and hydrogeological characteristics were loosely based on the western margin of the Great Artesian Basin (GAB, Australia). Here we use the western GAB purely as a demonstration aquifer to validate the new time constant solution for mixed aquifers (other similar aquifers could also have been chosen). Finally, t_{NE} values of 13 worldwide large aquifers have been estimated by using the solutions for mixed, fully confined and fully unconfined aquifers, depending on their characteristics.

2. Transient State

2.1. Transient State and Time Constant

[7] The GAB is one of the largest groundwater basins in the world. It covers more than 20% of the Australian continent. It is a multilayer aquifer system, mainly composed of sandstones, mudstones, and shales. The main aquifer, the Cadna-owie and equivalents (later called J aquifer), is artesian over a large portion of its extent [*Habermehl*, 1980; *Keppel et al*., 2013; *Love et al*., 2013a, 2013b]. Two principal groundwater flow directions have been identified in the main aquifer, one from northeast to southwest and one from northwest to southeast, with a convergent area near the Lake Eyre South (Figure 1). This present study is loosely based on the western GAB where the groundwater flow direction is mainly northwest to southeast. On the western GAB, the main natural discharge processes are springs and diffuse discharge [*Love et al*., 2013a] and the only recharge process occurring today is ephemeral river recharge [*Love et al*., 2013b]. These authors showed that the western GAB is not in balance between recharge and natural discharge, recharge being no more than 20% of the natural discharge. The study by *Love et al*. [2013b] clearly shows that, under the current climate, the western GAB is in a transient state.

[8] In such an aquifer, after a hydraulic perturbation, the hydraulic heads will slowly adjust to the new conditions until a new equilibrium is approached. This adjustment can be represented by an exponential function [*Schwartz et al*., 2009] characterized by a time constant τ which provides an estimation of the time required to reach a near-equilibrium [*Riley*, 1969; *Domenico and Schwartz*, 1998; *Alley et al*., 2002].

[9] Transient states have been studied mainly in cases of aquitard compaction after modification of the hydraulic heads in the adjacent aquifers [*Neuzil*, 1986; *Leake*, 1990; *Neuzil*, 1995]. In this situation, the time constant has been derived from Terzaghi's compaction theory and represents the time required for reaching more than 90% of the final consolidation [*Riley*, 1969; *Burbey*, 2001]. This is particularly important for aquitards submitted to mechanical compaction and where overpressuring may eventually occurs due to incomplete compaction. When such an overpressured aquitard is connected through its top and bottom boundaries to aquifer beds, its hydraulic pressure relaxes toward equilibrium through vertical fluid flow, with a time constant given by [*Riley*, 1969; *Leake*, 1990; *Burbey*, 2001]:

$$\tau_a = \frac{S_s (b/2)^2}{K_v} \tag{1}$$

where τ_a is the time constant for an aquitard (T), S_s is the specific storage (L^{-1}), b is the thickness of the aquitard (L), and K_v is the vertical permeability ($L\,T^{-1}$). In such low permeability aquitards, the time constant may be very large (on the order of 10^6 years) [*Neuzil*, 1986] and remnant abnormal pressures may persist for a long time after the end of the initial perturbation.

[10] On the contrary, aquifers characterized by a permeability much larger than that of aquitards are unlikely to present very long-term transient behaviors [*Neuzil*, 1986]. Nevertheless, some long-term transient behaviors (on the order of tens of thousands of years) have been identified in several aquifers [e.g., *Burdon*, 1977; *Lloyd and Farag*, 1978; *Houston and Hart*, 2004; *Jost et al*., 2007].

[11] Analytical expressions of these time constants for confined and unconfined aquifers have been proposed by *Domenico and Schwartz* [1998] and *Reilly and Harbaugh* [2004], respectively. *Domenico and Schwartz* [1998] defined the time constant for a homogeneous, isotropic and fully confined aquifer with a purely horizontal flow:

$$\tau_c = \frac{S_s L^2}{K_h} = \frac{SL^2}{T} \tag{2}$$

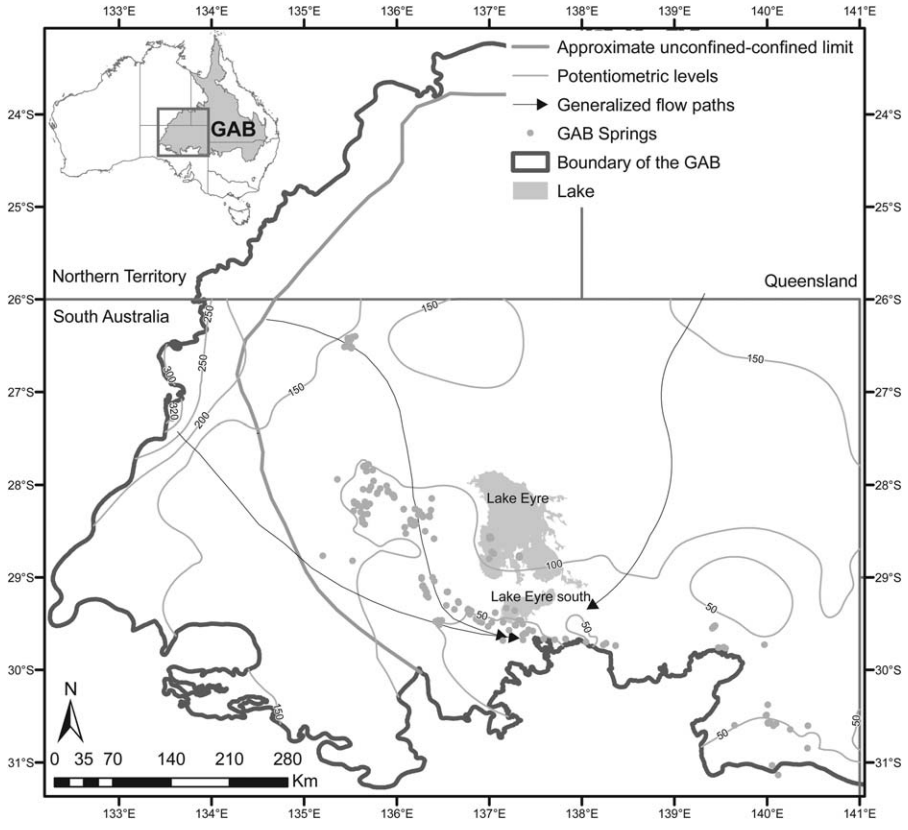

Figure 1. Hydrogeologic characteristics (unconfined-confined extent, potentiometric levels, generalized groundwater flow) of the western Great Artesian Basin used as an example for the study of large mixed aquifers.

where τ_c is the time constant for a confined aquifer (T), L is the aquifer length (L), K_h is the horizontal hydraulic conductivity (L T^{-1}), and S_s is the specific storage (L^{-1}). Multiplying these two quantities by the thickness of the (completely saturated) aquifer layer, one obtains the second equality of equation (2), where S is the storativity and T is the transmissivity (L^2 T^{-1}).

[12] For a homogeneous, isotropic and fully unconfined aquifer with a horizontal flow, a quite similar formula has been proposed [*Reilly and Harbaugh*, 2004; *Urbano et al*., 2004]:

$$\tau_u = \frac{S_y L^2}{T} \tag{3}$$

where τ_u is the time constant for an unconfined aquifer (T), T is an average transmissivity (see below), and S_y is the specific yield.

[13] Although equations (2) and (3) for the time constants of both confined and unconfined aquifers look quite similar, major differences in the hydraulic characteristics must be pointed out. In the case of an unconfined aquifer, the storage corresponds mainly to a variation on the level of the water table and the storage capacity is characterized by the specific yield. In the case of the confined aquifer, the storage capacity is mainly supplied by the possibility of porosity variation and water compressibility by some quasielastic deformation phenomena, the amplitude of which is very limited. Therefore, the specific yield S_y of an unconfined aquifer is generally much larger than the storativity S of a confined aquifer. Another important difference is that for unconfined aquifers, the transmissivity is a function of the saturated thickness of the aquifer whereas for confined aquifers, the transmissivity can be assumed independent of the pressure (or hydraulic head). As a consequence, in the latter case, the fluid pressure (or hydraulic head) satisfies a diffusion-type linear partial difference equation. Conversely, in the unconfined case, the partial equation becomes highly nonlinear [*de Marsily*, 1986].

[14] A common feature of equations (2) and (3) is that the length of the aquifer comes with a power of two. Thus for very large aquifers (hundreds of kilometers), long-term transient behaviors are likely to exist. However, this is less likely for confined aquifers than unconfined aquifers, due to the difference of several orders of magnitude in storativity between those two types of aquifers. As a result $\tau_c \ll \tau_u$ for aquifers of the same length L and characteristics.

[15] In the following, we will show how an aquifer (belonging to three types: either confined, unconfined, or mixed), once submitted to a sudden change of its recharge conditions, returns to a new equilibrium. A model of a subhorizontal aquifer layer of length L, which applies to the three cases (Figure 2), is defined in section 2.2. The relaxation toward equilibrium is characterized by t_{NE}, defined here as the time required for the initial hydraulic heads to be dissipated by 95% on average across the aquifer. For phenomena decreasing exponentially with a decay factor as $\exp(-t/\tau)$, $t_{NE} = 3\tau$ since $\exp(-3) \sim 0.05$.

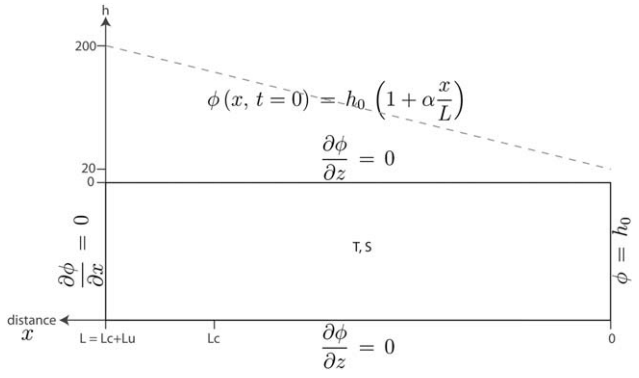

Figure 2. Conceptual model with initial and boundary conditions used in the analytical and numerical approaches. The initial condition varies between $h = 200$ m at $x = L$ and $h = 20$ m at $x = 0$. For the unconfined case, $h = 0$ corresponds to the bottom of the aquifer, therefore the saturated thickness varies from 200 to 20 m at $t = 0$ and equals 20 m at equilibrium ($t = \infty$) so that the transmissivity varies in space and time. Whereas for the confined case (represented here) $h = 0$ m coincides with the top of the aquifer, therefore the saturated thickness is constant as is the transmissivity. For the mixed aquifer analysis, L is divided in L_c and L_u, and the two conditions at the interface are continuous potential and flux.

[16] Although an average dissipation across the aquifer and a time of exp (−3) have been used as equivalents, in general this is an approximation. This is in part due to the consideration of real aquifers, initial perturbations are variable and different effects of variations in ratios of confined to unconfined aquifer lengths. Even with the 1-D model and analytical results proposed below for the complete range of mixed aquifer lengths from confined through to unconfined, this equivalence is not exact, but generally to within 95 ± 1.5%. Of course by modifying the time such that 3 is now $3 \pm \delta$, the 95% target can be achieved, but this makes the criteria problem specific and defeats the aim of a time constant, τ_m, in terms of aquifer properties and a simple exponential, exp (−3).

2.2. Time Constant τ_c and t_{NE} for a Confined Aquifer

[17] The case of a confined aquifer is a classical one [*Palciauskas and Domenico*, 1989]. For an homogeneous layer such as illustrated in Figure 2, it is convenient to use the Dupuit assumption [*Bear*, 1972; *de Marsily*, 1986] which states that for long aquifers the vertical component of the velocity can be neglected and the problem reduces to a 1-D one, along the horizontal distance x, where the hydraulic potential satisfies the diffusion equation:

$$D\frac{\partial^2\phi}{\partial x^2} = \frac{\partial\phi}{\partial t} \tag{4}$$

[18] Here D is the hydraulic diffusivity defined by $D = K/S_s = T/S$. The boundary conditions are $\phi = h_0$ at $x = 0$ and $\partial\phi/\partial x = 0$ at $x = L$. In the absence of recharge, the equilibrium state is one where the potential is constant and equal to h_0 for any x value. The assumed initial state is that, at $t = 0$, a large-scale disturbance occupies the whole aquifer space and may be described by a linear variation of the potential with x:

$$\phi(x, t=0) = h_0\left(1+\alpha\frac{x}{L}\right) \tag{5}$$

[19] Note that, since the boundary condition at $x = L$ is one of zero flow, the problem is exactly similar to that of an aquifer of length 2 L, with imposed potential at both ends, and with a triangular-shaped initial value ($\phi(x, t=0) = h_0(1+\alpha x/L)$ for $x \le L$ and $\phi(x, t=0) = h_0(1+\alpha(2L-x)/L)$ for $x \ge L$). The relaxation of ϕ from this initial state toward equilibrium $\phi(x, t=\infty)$ can be expressed mathematically as [*Carslaw and Jaeger*, 1959, p. 97]:

$$\phi_c(x,t) = h_0 + 8\alpha h_0 \sum_{n=1}^{\infty} \frac{(-1)^{n-1}}{(2n-1)^2\pi^2} \sin\left(\frac{(2n-1)\pi x}{2L}\right) \exp\left(\frac{-(2n-1)^2\pi^2 tD}{4L^2}\right) \tag{6}$$

[20] This relaxation is expressed as a series of terms decreasing exponentially as a function of time. Each term of this series corresponds to the relaxation of a specific mode n ($n = 1, 2, \ldots$) each one of them corresponding to a Fourier component (as a function of x) of the initial disturbance. Since the initial disturbance has a dominating large wavelength (i.e., its first harmonic for $n = 1$ is the largest), the first term of this series account for more than 80% even at the initial disturbance. The contribution of the next terms ($n = 2, 3 \ldots$) of the series vanishes very quickly as a function of time and harmonic rank (n). It is therefore justified to focus on the first term of the series, that is to say to neglect those for $n \ge 2$ and to write:

$$\phi_c(x,t) = h_0 + \frac{8\alpha h_0}{\pi^2} \exp\left(\frac{-\pi^2 tD}{4L^2}\right) \sin\left(\frac{\pi x}{2L}\right) \tag{7}$$

[21] This is the justification of the time constant τ_c given in equation (2), to within a factor $4/\pi^2$. Since $\exp(-3) \approx 0.05$, the time for returning to steady state (equilibrium) at 95% is, for any x, given by:

$$t_{NE} = 3 \times \frac{4L^2}{D\pi^2} = 3 \times \frac{4}{\pi^2}\tau_c \tag{8}$$

[22] In summary, it appears that, for a confined aquifer submitted to the initial and boundary conditions used in our model, $t_{NE} \sim 1.22\tau_c$. When examining the overall dissipation percentages, they are 96% at $x = L$, 93.7% at $x = 0$, 95% at $x = 0.7$ L, and with an average of 94.5%. These percentages show that although the 95% average and exp (−3) do not produce equivalence, nevertheless they are a good approximation to each other.

2.3. Time Constant τ_u and t_{NE} for an Unconfined Aquifer

[23] Modeling of an unconfined aquifer becomes highly nonlinear due to handling of its free, top surface. A standard analytical model is the Boussinesq equation [*Bear*, 1972]. A 1-D linearization of this equation is identical to

equation (4) with ϕ representing the height to the free surface from a fixed base and D_c being replaced by D_u. The solution equation (6) for the same perturbation and boundary conditions is then a solution for the unconfined aquifer as well. However, in order to handle the nonlinear situation, numerical estimations are necessary. We therefore made groundwater flow calculations using the numerical code MODFLOW96 [*McDonald and Harbaugh*, 1988; *Harbaugh and McDonald*, 1996] and the software Processing MODFLOW [*Chiang and Kinzelbach*, 1998]. This code is a three-dimensional finite difference code capable of simulating transient flow in porous media. The relevant governing equations and the mathematical basis for MODFLOW96 are discussed in *McDonald and Harbaugh* [1988] and *Harbaugh and McDonald* [1996].

[24] A homogeneous and isotropic aquifer is simulated as a 2-D cross section. For the unconfined case of interest here, the saturated thickness varies in the range from 200 m to 20 m (Figure 2). The same boundary conditions as for the confined case have been used: on the right side of the model (Figure 2), a head of 20 m is prescribed and a zero flux is prescribed on the left side. The initial conditions are those presented above and illustrated in Figure 2. The hydraulic perturbation simulated here is a cessation of the recharge producing a decay of the hydraulic heads with time. The final equilibrium state results in an homogeneous 20 m saturated thickness imposed by the right-hand side Dirichlet condition (h_0). Generic hydraulic conductivity and specific yield values for sandstones used in this model are, respectively, 1×10^{-6} m s^{-1} and 0.25 [*Domenico and Schwartz*, 1998].

[25] As previously mentioned, t_{NE} is defined as the time required for 95% of the perturbation to be dissipated, and more particularly when the whole aquifer is in near-equilibrium, then for all $x, h_{x,t} - h_0 \approx 0.05\mathrm{x}\left(h_{x,0} - h_0\right)$. As expected, results from the numerical models show that t_{NE} is not the same everywhere in the aquifer, the portion near the constant head boundary condition reaches near-equilibrium slightly more slowly. The variation of t_{NE} as function of x depends on the initial conditions, as well as on the boundary conditions of the model.

[26] In $\tau_u = SyL^2/T$ (equation (3)), the transmissivity is assumed constant whereas this is not the case in our numerical model, i.e., the transmissivity varies linearly with the aquifer saturated thickness (i.e., the hydraulic head) in space and time. It is then important to assess the relation between t_{NE} and τ_u for different transmissivities [see e.g., *de Marsily*, 1986]:

[27] 1. T_{max} is defined as the mean transmissivity for the initial conditions, $T_{max} = \frac{T_{x_0}^{t_0} + T_{x_L}^{t_0}}{2}$

[28] 2. T_{min} is defined as the mean transmissivity for the final conditions, $T_{min} = \frac{T_{x_0}^{t_f} + T_{x_L}^{t_f}}{2}$

[29] 3. T_{av} is defined as the arithmetic average transmissivity, $T_{av} = \frac{T_{x_0}^{t_0} + T_{x_L}^{t_0} + T_{x_0}^{t_f} + T_{x_L}^{t_f}}{4}$

[30] 4. T_{geo} is defined as the geometric average transmissivity, $T_{geo} = \sqrt[4]{T_{x_0}^{t_0} \times T_{x_L}^{t_0} \times T_{x_0}^{t_f} \times T_{x_L}^{t_f}}$

[31] 5. T_{har} is defined as the harmonic average transmissivity, $T_{har} = \frac{4}{\frac{1}{T_{x_0}^{t_0}} + \frac{1}{T_{x_L}^{t_0}} + \frac{1}{T_{x_0}^{t_f}} + \frac{1}{T_{x_L}^{t_f}}}$ where $T_{x_0}^{t_0}$ is the transmissivity at $x = 0$ and $t = 0$, $T_{x_L}^{t_0}$ is the transmissivity at $x = L$ and $t = 0$, $T_{x_0}^{t_f}$ is the transmissivity at $x = 0$ and $t = final$, and $T_{x_L}^{t_f}$ is the transmissivity at $x = L$ and $t = final$. Note that in our case since $\phi_c = h_0$ at $x = 0$ the transmissivity at $x = 0$ is constant over time, therefore $T_{x_0}^{t_0} = T_{x_0}^{t_f}$.

Table 1. Comparison of τ_u for Five Different Transmissivities (Maximal, Minimal, Arithmetic Average, Geometric Average, and Harmonic Average) and t_{NE}

Transmissivity	t_{NE}/τ_u
T_{max}	3.6
T_{min}	0.7
T_{av}	2.1
T_{geo}	1.2
T_{har}	0.8

[32] The comparison of t_{NE} and τ_u for different transmissivities shows that depending on what transmissivity is used, t_{NE} can be estimated from τ_u using a correction factor varying between 0.7 and 3.6 (Table 1). Although, the order of magnitude given by $t_{NE} \sim \tau_u$ is quite correct, the range of corrective factors highlights the difficulty in prescribing transmissivity values in unconfined aquifers. Moreover, often in case studies only a few transmissivity values are available and then the calculated average may be different from what has been presented here. Therefore, the analytically determined time constants in such systems are best viewed as indicative or relative values rather than absolute or precise values.

3. Time Constant for a Mixed Aquifer

[33] In the previous section, the time constants applicable to homogeneous aquifers with a single hydrodynamical behavior (i.e., confined or unconfined) have been considered. It remains to study the case of a mixed aquifer, i.e., unconfined in one part (and possibly fed by rainfall) which becomes confined by an upper aquitard in the other part. This mixed aquifer juxtaposition and the situation where recharge of the unconfined part stops suddenly are typical of many hydrogeological situations. This occurs, for example, in the GAB.

[34] As previously stated, major differences between the confined part of the aquifer and its unconfined part lie in their different storage capacities and also in the fact that, for an unconfined aquifer, the diffusion of hydraulic head is submitted to nonlinear effects because the transmissivity strongly depends on the head itself. However, in order to obtain an analytical solution, a linearized approach is required.

[35] Therefore, two modeling approaches, analytical and numerical, have been developed for estimating the time constant in a mixed aquifer. The analytical approach provides two new formulae for the time constant of a mixed aquifer. In this approach, the differences between the confined and the unconfined parts of the aquifer are simplified and restricted to only differences in storage coefficients. The second approach is a numerical one, which fully takes into account the nonlinearities occurring in the problem, and is then applied in order to validate the new analytical formulae.

3.1. Analytical Approach

[36] In the conceptual model, illustrated in Figure 2, an aquifer with two continuous parts is considered, one

confined of length L_c and the other unconfined of length L_u. Both portions are assumed to satisfy a linear diffusion equation, the saturated thickness and transmissivity are thus constant in the unconfined part as well as in the confined part. The important feature characterizing the unconfined part is that its storage coefficient (S_u) is normally much larger by a factor of some 10^3 than that of the confined part (S_c). A further assumption must be made in order to develop the analytical solution. It is assumed that the variation in hydraulic heads only depends on the horizontal distance x. The lateral dimension perpendicular to the x-z plane of Figure 2 has been neglected by performing the analysis in cross section. The z-dimension may be neglected based on the Dupuit assumption [*de Marsily*, 1986], which states that for a long and relatively thin aquifer, the vertical component of the velocity can be neglected. These simplifications allow us to reduce the groundwater flow problem to 1D.

[37] With these two assumptions, the following two diffusion equations are obtained, where subscript u indicates the parameters for the unconfined portion and c for the confined one:

$$\text{unconfined portion}, L_c < x < L: \quad D_u \frac{\partial^2 \phi_u}{\partial x^2} = \frac{\partial \phi_u}{\partial t}, \ \text{where } D_u = \frac{T_u}{S_u} \tag{9}$$

$$\text{confined portion}, 0 < x < L_c: \quad D_c \frac{\partial^2 \phi_c}{\partial x^2} = \frac{\partial \phi_c}{\partial t}, \ \text{where } D_c = \frac{T_c}{S_c} \tag{10}$$

where, in the confined and unconfined portion, $D_{u,c}$ are the diffusivity coefficients ($L^2\ T^{-1}$), $\phi_{u,c}$ are the hydraulic heads (L), x is the distance in the x direction from the confined end (L), and t is the time (T). The parameter f defined as $f = S_c/S_u$ is used to characterize the ratio between the specific storage of both aquifer portions. The specific storage of the unconfined aquifer (roughly the drainage porosity, or specific yield) is much larger than that of the confined one (depending on the volumetric compressibility). Therefore $S_u \gg S_c$ and $f \ll 1$ (typically 10^{-3}).

[38] The aquifers are assumed to be homogeneous and isotropic. Then, as the saturated thickness of the unconfined portion is assumed constant, i.e., groundwater flow described by a linear diffusion equation, the transmissivity of the aquifer is constant in space and time. Therefore, T_u equals T_c and $D_u/D_c = f$.

[39] As in sections 2.2 and 2.3, the initial conditions for the hydraulic heads are:

$$\phi(x, t = 0) = h_0\left(1 + \alpha \frac{x}{L}\right) \tag{11}$$

where h_0 is the prescribed hydraulic head at $x = 0$ (Figure 2). The boundary conditions are a prescribed head ($\phi_c(0, t) = h_0$) on the right side and a zero flux (i.e., $\frac{\partial \phi_u}{\partial x}(L, t) = 0$) on the left one. At the interface between the unconfined and confined part, the hydraulic potential and flux are continuous.

[40] An analytical solution to this problem has been obtained by using the Laplace transform of the diffusion equations. The solution of the problem is developed in Appendix A: ϕ is defined in both compartment as:

$$\phi_c = h_0 + 2\alpha h_0 \sqrt{f} \sum_{n=1}^{\infty} \frac{\exp\left(\frac{-L^2\beta_n^2 t}{D_c}\right)\left\{\sin\left(\beta_n \frac{x}{L}\right)\sin\left(\frac{\beta_n}{\sqrt{f}}\frac{L_u}{L}\right)\right\}}{\beta_n^2\left\{1 - \frac{L_c}{L}(1-f)\cos^2\left(\frac{\beta_n}{\sqrt{f}}\frac{L_u}{L}\right)\right\}\cos\left(\beta_n \frac{L_c}{L}\right)} \tag{12}$$

$$\phi_u = h_0 + 2\alpha h_0 f \sum_{n=1}^{\infty} \frac{\exp\left(\frac{-L^2\beta_n^2 t}{D_c}\right)\cos\left(\frac{\beta_n}{\sqrt{f}}\left(1 - \frac{x}{L}\right)\right)}{\beta_n^2\left\{1 - \frac{L_c}{L}(1-f)\cos^2\left(\frac{\beta_n}{\sqrt{f}}\frac{L_c}{L}\right)\right\}} \tag{13}$$

where β_n are the positive solutions of the equation in β:

$$\Delta(\beta) = \sqrt{f}\cos\left(\frac{L_u\beta}{L\sqrt{f}}\right)\cos\left(\frac{L_c\beta}{L}\right) - \sin\left(\frac{L_u\beta}{L\sqrt{f}}\right)\sin\left(\frac{L_c\beta}{L}\right) = 0 \tag{14}$$

[41] The successive root values $\beta_{1,2,\ldots}$ can be found numerically using Newton's method. Different approximations to the dominant, first and also smallest root can be found as discussed in Appendix A. One approximation that is based on the fact that f is small will be used because it covers the values of f and L_c/L for the aquifers considered in this paper. Another that is based on a small β expansion of Δ (β) will be presented for completeness to cover other possible values of f and L_c/L.

[42] In Appendix A, it is shown that, for small values of f—the ratio of S_c/S_u—the first and smallest root β_1 is very well approximated by β_{10}:

$$\beta_{10} = \sqrt{\frac{fL^2}{L_u\left(L_c + \frac{L_u}{2}\right)}} \tag{15}$$

so that the time variation of the potential can be approximated by $\exp(-t/\tau_m)$ with τ_m given by:

$$\tau_m = \frac{D_c L^2}{\beta_{10}^2} = \frac{D_c L^2}{\frac{fL^2}{L_u\left(L_c + \frac{L_u}{2}\right)}} = \frac{S_u L_u}{T}\left(L_c + \frac{L_u}{2}\right) \tag{16}$$

[43] Therefore in the case of a mixed aquifer using our definition of t_{NE}, we can evaluate t_{NE}, the time for returning to steady state at 95% by:

$$t_{NE} \approx \frac{3S_u L_u}{T}\left(L_c + \frac{L_u}{2}\right) \tag{17}$$

[44] This is our basic formula applied in this paper for a mixed aquifer. Its singular aspect is that the storativity of the confined aquifer S_c disappears, whereas the effective length (by comparison with equations (2) and (3) for single aquifers) is something like a harmonic average of the lengths of the unconfined portion (L_u) and the confined portion (L_c), this latter length being "corrected" by half L_u. However, it is clear that this relation breaks down for $L_u = 0$: the time constant derived from equation (16) is then 0. In fact for $L_u = 0$, the aquifer becomes

homogeneous and the relevant time constant is therefore given by equation (8).

[45] As developed in Appendix A, the expressions (15) and (16) are derived from an approximation which is valid for small f values and nonvanishing L_u values (ratio $f/\xi_u \leq 0.3$, where $\xi_u = L_u/L$). This is the case for situations studied in the present work but for extension of the work toward more flexible conditions on f and L_u, it is necessary to obtain better approximations of the root β_1. These improved solutions are developed in Appendix A, where solutions displaying no singularity near $L_u = 0$ and remaining very precise with respect to the definition of β_1 are proposed. One of these solutions of sufficient accuracy is:

$$\beta_{12} = \sqrt{\frac{f\left(a_2 - \sqrt{a_2^2 - 4a_4}\right)}{a_4}} \tag{18}$$

where a_2 and a_4 are given by

$$a_2 = \frac{L_u^2 + 2L_uL_c + fL_c^2}{L^2} \tag{19}$$

$$a_4 = \frac{L_u^4 + 4L_u^3L_c + 6fL_u^2L_c^2 + 4fL_uL_c^3 + f^2L_c^4}{L^4} \tag{20}$$

[46] The scaling time constant associated with β_{12} is:

$$\tau_{m2} = \frac{L^2}{D_c\beta_{12}^2} = \frac{a_4L^2}{\left(a_2 - \sqrt{a_2^2 - 4a_4}\right)D_u} \tag{21}$$

[47] Besides the mathematical approximation of equation (17), many physical assumptions—such as the confusion between an unconfined aquifer and a confined one with large storativity—have been used to derive this formula. It is thus important to assess its robustness using comparisons with numerical computations.

[48] The effect of extra dimensionality (i.e., 2-D or 3-D flow) on the time constant is complex and depends on the flow regime, which is controlled by factors including aquifer geometry and boundary conditions, and also heterogeneity and anisotropy, etc. Indeed, it appears that when flows are convergent, then the time constant is expected to be larger than that given by the 1-D case. Conversely, when the flows are divergent, the time constant is expected to be smaller than that given by the 1-D case. These conclusions have been drawn from preliminary 2-D calculations in Cartesian coordinates following the analysis of *Carslaw and Jaeger* [1959, pp. 173–175]. They have also been verified with further calculations using cylindrical coordinates where the flow is either directed toward the center (convergent) or outward (divergent). Therefore, the effect of spatial dimensionality on the value of the time constant depends on both the geometry of the aquifer and more importantly on the position and type of the boundary conditions. 2-D or 3-D effects may therefore result in either an increase of the time constant for convergent flow or a decrease of the time constant for divergent flow. In the case of a complex aquifer, the time constant can be seen as an integrative property which characterizes its transient behavior. The proposed 1-D approximation is only a simple and preliminary guide to the description of transient aquifer behavior. More detailed analyses and modeling will usually be required for a rigorous assessment of the transient behavior of aquifer systems, especially those with complex flows, geometries, boundary conditions, and heterogeneity.

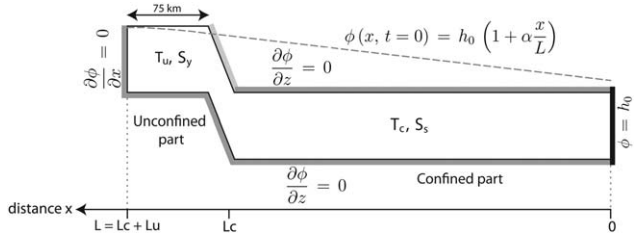

Figure 3. Two-dimensional cross section of the conceptual model of a mixed aquifer studied by the numerical approach. The initial and boundary conditions are the same as those used in the analytical approach. In this model, T varies on the unconfined portion as a function of h (x,t). The unconfined portion at the initial state is 75 km long and the discharge area covers a distance of 50 km.

3.2. Numerical Approach

[49] The purpose of the numerical approach was to verify the validity of the assumptions used for obtaining the time constant formula (equation (16)) by comparison with the results of a numerical model taking into account or not the nonlinearities, i.e., variations of the saturated thickness in the unconfined portion. The conceptual model is a homogeneous single layer with both unconfined and confined portions and a discharge area (Figure 3).

[50] This numerical model is loosely based on the geometrical and hydrogeological characteristics of the western GAB. The geology and hydrogeology of the J aquifer are however very complex (faults, leakages, etc.)[*Keppel et al.*, 2013]. The purpose of this numerical model is not to represent the exact geology or hydrogeology of the J aquifer nor is it to simulate water fluxes. Here we use its broad characteristics in a general way to give some reality to the numerical model used, such as the size of the groundwater system. To do this we use the approximate geometry (length and thickness) of the groundwater flow system along the western GAB with the average hydraulic characteristics of the J aquifer [*Keppel et al.*, 2013; *Love et al.*, 2013a, 2013b].

[51] On the western GAB, the J aquifer has a mean thickness of 200 m. It is partly confined by a clay layer. The water flows over a distance of 500 km, from the outcrops (~75 km long) of the J aquifer on the western margin to a discharge area near the Lake Eyre (Figure 1). The grid spacing across the model domain was $\Delta x = 1$ km, the y dimension is neglected by performing a cross-section analysis. A grid convergence test was performed with a spatial discretization of $\Delta x = 0.5$ km. The results obtained were the same, validating the accuracy of the coarse mesh, which has been used for all the simulations. The recharge area (75 km on the western part of the model) was modeled as an unconfined portion of the aquifer. The discharge area was modeled by a constant hydraulic head condition

Table 2. Hydrodynamic Parameter Values Used in the Calculations (From *Welsh* [2007])

Parameters	Ref	Min	Max
K (m s^{-1})	8.1×10^{-5}	8.1×10^{-8}	8.1×10^{-2}
S_s (m^{-1})	5.5×10^{-6}	5.5×10^{-8}	5.5×10^{-4}
S_y	0.25	0.05	0.25

prescribed at the right side of the model. A constant head of 20 m above the top of the layer, similar to measurements near Lake Eyre (discharge area, Figure 1), was used. The top and bottom of the model were assigned no flow boundary conditions (Figure 3), representing impermeable confining layers above and below the J aquifer. Hydraulic parameters for the GAB are available [*Welsh*, 2007], the range and the mean values, which were used in the numerical model, are given in Table 2.

[52] In this study, the transient state is caused by a change in the boundary condition of the unconfined portion (left side of the model), assumed to be related to a variation of recharge due to climate change. Indeed, the late Quaternary period has undergone several large glacial-interglacial changes with 100 kyr cycles [*Imbrie et al*., 1992]. The present interglacial period started at the Pleistocene-Holocene transition (10 kyr ago). It is assumed that the Pleistocene in Australia was wetter than present [*Kershaw and Nanson*, 1993]. The climate scenario used in this study assumes that before the Pleistocene-Holocene transition, the recharge was sufficiently important to maintain a high water level in the unconfined part of the conceptual model (Figure 3). At the end of the Pleistocene, the groundwater system is assumed to be in steady state, with a water level close to the ground surface on the unconfined portion of the model. During the whole Holocene, it is assumed that no recharge occurs at all. As a result, the change in boundary conditions is represented by a cessation of recharge at the Pleistocene-Holocene transition, i.e., from 10 kyr BP. Thus, an initial steady state with a high water level in the unconfined part was used as initial hydraulic heads for the transient simulations. Transient simulations were run with 3760 time steps to cover a simulation time over 1.9×10^6 years. The time-step size is not the same throughout the simulation. At the beginning of the simulation, the time step equals 1 year and increases nonregularly (different stress periods) to time steps of 1.0×10^5 years at the end of the simulation. The groundwater flow equations have been solved with the code MODFLOW using an implicit scheme (Strongly Implicit Procedure solver) [*Stone*, 1968; *McDonald and Harbaugh*, 1988].

3.3. Comparison Between Analytical and Numerical Approaches

[53] A first test was to compare the results of the analytical mixed aquifer solution with the mixed numerical model (MODFLOW) run with the assumption that the transmissivity is constant and does not depend on the saturated thickness of the aquifer, i.e., the hydraulic head. The results (not shown) give almost identical results, thus showing that the exact analytical solution is valid.

[54] We then ran MODFLOW with the transmissivity as a linear function of the saturated thickness, to represent a real unconfined aquifer. The analytical mixed aquifer solution is of course used with a constant transmissivity assumption. We thus measure the error made with the analytical solution when neglecting the transmissivity variation. The results obtained from the numerical model and from the new time constant for mixed aquifer for different hydraulic parameters are compared in Figure 4. For the calculations of the time constant, 87 and 363 km were used, respectively, for the lengths of the unconfined and confined parts (L_u, L_c). Those lengths correspond to the extent of the unconfined and confined parts of the near-equilibrium state, i.e., at t_{NE}. Moreover, for the calculation of the time constant, only one value of transmissivity was available and this was used.

[55] This comparison between t_{NE} and $3\tau_m$ (Figure 4) shows good agreement (mean error less than 10%) for different values of hydraulic conductivity, specific yield and specific storage. This agreement demonstrates the validity of using the analytical time constant for mixed aquifers (equation (16)) to estimate the time to reach a near-equilibrium in such aquifers, i.e., $t_{NE} = 3\tau_m$.

[56] For the mixed model, the results are not intended to simulate actual conditions of the western portion of the GAB but to provide evidence that at present this kind of system is expected to be unsteady and displays a transient behavior since $3\tau_m$ (52 kyr for the reference parameters) is larger than the time since the last hydrodynamic perturbation occurred (10 kyr). Moreover, these results suggest that high modern hydraulic heads can be explained by recharge events that occurred 10 kyr ago and possibly even older climate conditions since the perturbation is dissipated in more than 50 kyr. This result suggests that large aquifers with an

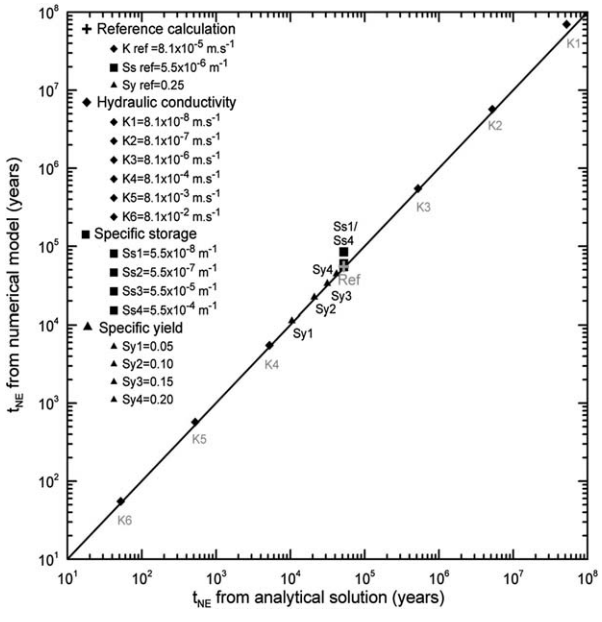

Figure 4. Comparison between t_{NE} obtained from the numerical approach and $\tau_m(t_{NE} = 3\tau_m)$ obtained with equation (17). The reference calculation has been done using the GAB hydrodynamic parameters [*Welsh*, 2007]. Different values of hydraulic conductivity, specific storage and specific yield have been used to validate the solution formula of τ_m for a broad range of parameters.

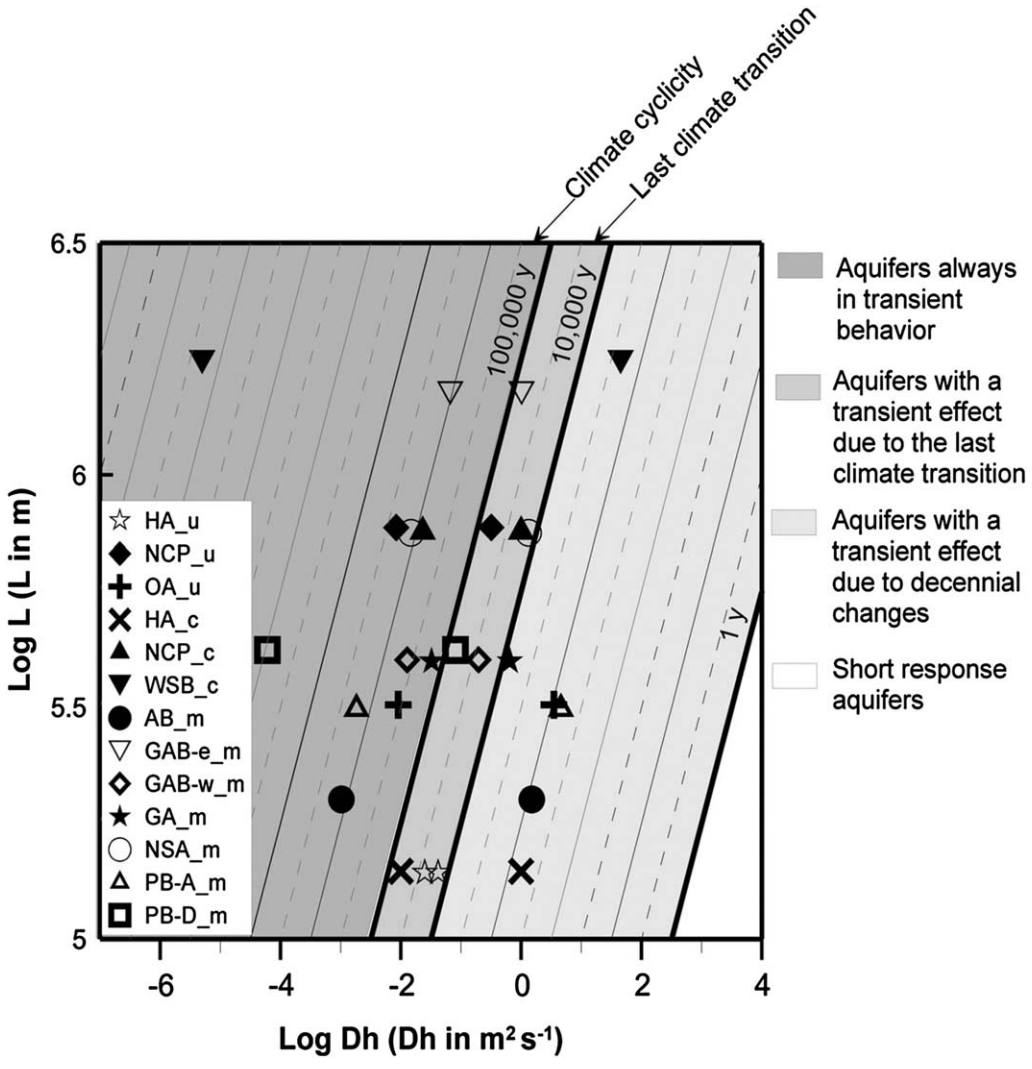

Figure 5. Time constant in years (logarithmic scale) as a function of the log of the hydraulic diffusivity (m^2 s^{-1}) and the log of the aquifer length (m). The last climate transition refers to the Pleistocene-Holocene transition, 10 kyr ago. The climate cyclicity refers to the mean time period of the climate cycle, i.e., 100 kyr since 0.9 Ma. The subscript u means that the aquifer is a fully unconfined aquifer and then equation (3) has been used to estimate the time constant. The subscript c means confined and equation (8) has been used to calculate the time constant. Finally, the subscript m means mixed and then the new solution (equation (17)) has been used to estimate the time constant. Aquifer abbreviations are: HA: Hungarian Aquifer, NCP: North China Plain, OA: Ogallala Aquifer, WSB: Western Siberia Basin, AB: Aquitaine Basin, GAB-e: Great Artesian Basin east, GAB-w: Great Artesian Basin west, GA: Guarani Aquifer, NSA: Nubian Sandstone Aquifer, PB-A: Albian in Paris Basin, and PB-D: Dogger in Paris Basin.

unconfined part are likely not in equilibrium with the modern climate and that at least a part of the present hydraulic heads are resulting from a long-term transient behavior inherited from wetter palaeoclimates. The time to reach near-steady state for this kind of aquifer suggests that the current hydraulic heads are the result of both current and past hydrodynamic conditions.

[57] In this present study, only the effect of a recharge cessation was investigated as perturbation of the hydrodynamic boundary conditions. Of course, other processes such as erosion, sedimentation, coastline modification, or eustatic-level change lead to a change of the discharge level [*Custodio*, 2002] and can also lead to and contribute to long-term transient effects. Moreover, only the case of a one-side hydraulic perturbation has been investigated. Although a particular perturbation (linear) has been exemplified, it is not expected that other types of large wavelength initial conditions would produce significantly different large time analytical behavior (see Appendix A).

4. Estimation of t_{NE} for Several Large Aquifers in the World

[58] Some theoretical calculations of τ were performed for different length (L, in m) and hydraulic diffusivity (D_h, m^2 s^{-1}) values (Figure 5). The following equation was used:

Table 3. Hydrodynamic Parameter Values for Different Large Aquifers in the World: The Eastern and Western Part of the GAB (GAB-e and GAB-w, Respectively), the Guarani Aquifer (GA), the Nubian System Aquifer (NSA), the Aquitaine Basin (AB), the Albian and Dogger in the Paris Basin (PB-A and PB-D, Respectively), the Hungarian Aquifer (Unconfined and Confined Aquifers, HA-u and HA-c, Respectively), the Western Siberia Basin (WSB), the North China Plain (Unconfined and Confined Aquifers, NCP-u and NCP-c), and the Ogallala Aquifer (OA)

					T (m^2 s^{-1})		S		Sy		3τ (years)	
Aquifers	Type	L_c (km)	L_u (km)	b (m)	Min	Max	Min	Max	Min	Max	Min	Max
GAB-e[a]	m	1450	50		1.5×10^{-3}	1.0×10^{-2}	2.5×10^{-4}	5.0×10^{-4}	0.10	0.23	7.7×10^{4}	1.2×10^{6}
GAB-w[a]	m	325	75		1.5×10^{-3}	1.0×10^{-2}	2.5×10^{-4}	5.0×10^{-4}	0.10	0.15	2.9×10^{4}	4.4×10^{5}
GA[b,c]	m	320	80		1.0×10^{-5}	1.0×10^{-4}	1.0×10^{-6}	1.0×10^{-3}	0.10	0.20	8.7×10^{3}	1.8×10^{5}
NSA[d]	m	530	220		3.0×10^{-3}	1.0×10^{-1}	2.0×10^{-4}	3.3×10^{-3}	0.10	0.27[m]	1.6×10^{4}	1.5×10^{6}
AB[e]	m	180	20		1.0×10^{-4}	3.2×10^{-2}	6.0×10^{-5}	4.0×10^{-4}	0.07	0.34	8.9×10^{2}	1.3×10^{6}
		L_c (km)	L_u (km)	b (m)	K (m s^{-1})		Ss (m^{-1})		Sy		3τ (years)	
PB-A[f,g]	m	300	20	100	1.0×10^{-6}	1.0×10^{-3}	1.0×10^{-4}	5.0×10^{-4}	0.12	0.30	1.7×10^{3}	2.7×10^{6}
PB-D[f,g]	m	390	30	250	1.0×10^{-8}	1.0×10^{-5}	5.0×10^{-5}	5.0×10^{-4}	0.15	0.20	1.5×10^{5}	1.7×10^{8}
HA[h]	u		140	750	1.0×10^{-5}				0.18	0.30	4.5×10^{4}	7.5×10^{4}
HA[h]	c	140			1.0×10^{-6}		1.0×10^{-6}	1.0×10^{-4}			1.9×10^{3}	1.9×10^{5}
WSB[i]	c	1750			5.0×10^{-9}	4.5×10^{-5}	1.0×10^{-6}	1.0×10^{-3}			6.5×10^{3}	5.9×10^{10}
NCP[j,k]	u		770	60	2.1×10^{-5}	8.0×10^{-4}			0.15		1.8×10^{5}	6.8×10^{6}
NCP[j,k]	c	770			2.3×10^{-5}	1.0×10^{-4}	1.0×10^{-4}	1.0×10^{-3}			5.6×10^{4}	2.4×10^{6}
OA[l]	u		320	200	1.0×10^{-5}	7.0×10^{-4}			0.04	0.22	2.7×10^{3}	1.1×10^{6}

[a] *Welsh* [2007].
[b] *Bonotto* [2006].
[c] *Kimmelmann e Silva et al*. [1989].
[d] *Sefelnasr* [2007].
[e] *Douez* [2007].
[f] *Jost* [2005].
[g] *Marty et al*. [1993].
[h] *Tóth and Almàsi* [2001].
[i] *Cramer et al*. [1999].
[j] *Chen et al*. [2004].
[k] *Han* [2008].
[l] *Nativ and Smith* [1987].
[m] *Anderson and Woessner* [1992].

$$\tau = \frac{L^2}{D_h} \tag{22}$$

[59] Depending on whether the aquifer is confined or unconfined, D_h is defined as T/S or T/Sy, respectively. The purpose of Figure 5 is to give some guidelines about the large values of the time to near-equilibrium. In Figure 5, four aquifer behaviors can be characterized as a function of the value of their times to near-equilibrium:

[60] 1. short response time aquifers with a $\tau < 1$ yr, with a possible transient behavior resulting from seasonal climate variations;

[61] 2. aquifers with a τ ranging between 1 yr and 10 kyr, with a possible transient behavior resulting from decennial climate changes as e.g., the Pacific Decadal Oscillation [*Alley et al*., 2002];

[62] 3. aquifers with a $\tau > 10$ kyr, in which the hydraulic heads result at least from the present and Pleistocene hydrodynamic boundary conditions;

[63] 4. aquifers with a $\tau > 100$ kyr, which is the length of a Milankovitch's cycle since the last 1 Ma [*Tiedemann et al*., 1994; *Naish et al*., 1998]. For this group, these results suggest that aquifers are rarely expected to be in steady state with respect to their hydraulic behavior.

[64] The t_{NE} for 13 large aquifers in the world have been estimated. From those aquifers, the Great Artesian Basin east and west (Australia), the Dogger and Albian aquifers in the Paris Basin (France), the Nubian Sandstone System (Egypt-Libya-Chad-Sudan), the Aquitaine Basin (France), and the Guarani Aquifer (Brazil-Paraguay-Uruguay-Argentina) are characterized by unconfined parts of the aquifers on the borders of their basins. The Hungarian Aquifer and the Western Siberia Basin (Russia) have shallow unconfined aquifers and deep totally confined aquifers. The North China Plain has unconfined and confined aquifers. The Ogallala Aquifer in the Southern High Plains (USA) is a large unconfined aquifer.

[65] For all these aquifers, t_{NE} values were calculated from equations (8), (3), or (17) according to the confined, unconfined, or mixed characteristics of the aquifers. The parameter values used for these calculations are summarized in Table 3 and the minimum and maximum value of t_{NE} for each aquifer is shown in Figure 5. For the mixed aquifers, an equivalent hydraulic diffusivity had to be used to accurately represent the t_{NE} obtained from equation (17). For example, for the GAB-e with the L and D_h given in Table 3 and plotted in Figure 5, $3\tau_m$ will range between 5 and 3×10^4 kyr, instead of 70 and 1×10^3 kyr obtained from the solution formula (equation (17)). So an equivalent D_h allowing to reproduce the $3\tau_m$ values obtained from equation (17) was used.

[66] The t_{NE} values obtained for all the aquifers range between 0.7 kyr and 2.4×10^7 kyr. Therefore, all these aquifers may present a long transient behavior after a

hydraulic perturbation. The results shown n Figure 5 suggest that probably all these large aquifers are not in equilibrium with their current boundary conditions. Moreover, for all these aquifers having their upper $t_{NE} > 100$kyr, they are likely to have never been in steady state and their current transient behaviors could be the result of several climate cycles.

[67] The t_{NE} values obtained for the Aquitaine Basin (200 km long, circles in Figure 5) or for the Hungarian Aquifer (140 km, white stars—unconfined—and triangles—confined—in Figure 5) range between 0.8 kyr and 1.3×10^3 kyr. These results suggest that aquifers smaller than 100 km may also have long-term transient behaviors, on the order of 10 kyr. In these systems, transient flows will be remnant from the last climate transition. This conclusion is in agreement with the time constant of 8 kyr found by *Schwartz et al*. [2009] for a 39 km long aquifer in USA.

[68] Long-term transient behavior may exist in fully confined aquifers. Indeed, t_{NE} values for the fully confined aquifers studied here (Western Siberia Basin, North China Plain, Hungarian Aquifer) vary between 0.8 kyr and 2.4×10^7 kyr. These values suggest that these confined aquifers are in disequilibrium with their current boundary conditions.

[69] Some large aquifers are not in arid or semiarid regions (Paris Basin, Aquitaine Basin, Western Siberia Basin, and Hungarian Aquifer). In the current temperate regions, the glacial periods were characterized by possible permafrost, which stopped the recharge mechanism [*Beyerle et al*., 1998; *Heathcote and Michie*, 2004; *Jost et al*., 2007]. At the Pleistocene-Holocene transition, the disappearance of this permafrost caused the recharge mechanism to restart and a transient flow started until reaching a new steady state with higher hydraulic heads.

5. Conclusions

[70] In this paper, a new solution to estimate the time to reach a near-equilibrium state in mixed aquifers has been proposed and validated. This new solution was obtained using Laplace transforms to solve the flow equation of a conceptual model of mixed aquifers, i.e., having adjacent unconfined and confined portions. The validation of this solution was performed by comparison with numerical results. The numerical model used in this study was based on a generic representation of the western portion of the Great Artesian Basin in Australia. It should be remembered here that the purpose of the model was not to reproduce exactly the groundwater flow of the GAB, but to estimate values of the time to reach a near-equilibrium t_{NE} and to validate the new solution formula. After validation, the new solution formula for mixed aquifers and the solutions for fully confined and fully unconfined aquifers were used to assess the t_{NE} of several large aquifers in the world.

[71] The analyzes performed in this paper show that large aquifers may present long-term transient behaviors, which is an important result since it is usually assumed that aquifers quickly adjust to any hydraulic perturbation. Therefore, the estimation of t_{NE}, based on the proposed analytical expressions for τ_c, τ_u, or τ_m, should be more systematically and routinely applied in the study of large aquifers in order to properly understand their hydrodynamic state.

Appendix A: Solution by Laplace Transforms of a Problem of Contiguous Aquifers

A1. Assumptions and Definitions

[72] Consider an aquifer (along the horizontal direction x, infinitely wide in the orthogonal horizontal direction y) composed of two contiguous compartments indexed by c and u (confined and unconfined) (Figure 2). Assume that the slope and thickness are sufficiently small in both compartments so that, in both sections, the hydraulic potential satisfies the 1-D diffusion equation. In the compartment c, with length L_c, the hydraulic potential $\phi = \phi_c$ follows the standard diffusion equation with a homogeneous transmissivity T, a storage coefficient S_c, and, therefore, a diffusivity $D_c = T/S_c$. In the neighboring compartment u, with length L_u, the transmissivity T is assumed to be the same, but the storage coefficient S_u is different (much larger than S_c) as is the diffusivity $D_u = T/S_u$. In the latter compartment, the hydraulic potential $\phi = \phi_c$ also follows the diffusion equation with diffusivity $D_u \ll D_c$.

[73] Mathematically, the potential ϕ obeys the equation:

$$D\frac{\partial^2\phi}{\partial x^2} = \frac{\partial\phi}{\partial t} \tag{A1}$$

with $D = D_c$ in the confined compartment $(0 < x < L_c)$ and $D = D_u$ in the unconfined one $(L_c < x < L = L_c + L_u)$ whereas, at the interface $x = L_c$, the potential ϕ is continuous, as well as the hydraulic flow $T\partial\phi/\partial x$, so that:

$$\text{at } x = L_c,\ \phi_u = \phi_c, \text{ and } T\partial\phi_u/\partial x = T\partial\phi_c/\partial x$$

[74] The other boundary conditions are that

$$\text{at } x = 0, \text{ the potential is prescribed}: \phi_c = h_0$$
$$\text{at } x = L = L_u + L_c, \text{ the flow is null, so that } \frac{\partial\phi_u}{\partial x} = 0.$$

[75] Since it is assumed that there is no producing source in the system, the boundary conditions impose that the steady-state potential equals h_0 for any x. Now let us impose an initial condition, for time $t = 0$, corresponding to a large-scale disturbance of the system: at $t = 0$, the potential in both compartments is assumed to vary linearly with x: $\phi(x, t = 0) = h_0(1 + \alpha x/L)$.

[76] When t increases, the potential $\phi(x,t)$ relaxes toward the steady state $\phi(x, t = \infty) = h_0$. For large times, by analogy with the solution of the confined aquifer presented in section 2.2, the relaxation behavior is expected to be characterized by an exponential decay. The problem is to define the coefficient attached to the time variable.

[77] Nondimensional variables are defined by:

$$\xi = x/L, \xi_u = L_u/L, \text{ therefore } \xi_c + \xi_u = 1, t^* = D_c t/L^2.$$

[78] The difference between the two compartments is characterized by a fraction f: $f = D_u/D_c = S_c/S_u$. Since $S_c \ll S_u, f$ is very small.

[79] In the two compartments u and c, the diffusion equations become:

$$\frac{\partial^2 \phi_c}{\partial \xi^2} = \frac{\partial \phi_c}{\partial t^*} \tag{A2}$$

$$\frac{\partial^2 \phi_u}{\partial \xi^2} = \frac{D_c}{D_u}\frac{\partial \phi_u}{\partial t^*} = \frac{1}{f}\frac{\partial \phi_u}{\partial t^*} \tag{A3}$$

[80] The boundary conditions are that

at $\xi = 0, \phi_c = h_0$
at $\xi = 1, \partial\phi_u/\partial\xi = 0$
at $\xi = \xi_c$, the potential is continuous $(\phi_c = \phi_u)$
as well as the flux $(T\partial\phi_c/\partial\xi = T\partial\phi_u/\partial\xi)$

A2. Solution by Laplace Transforms

[81] Laplace transforms of the previous equations are performed. Let ψ (index u or c) be the Laplace transform of ϕ (index u or c) defined by:

$$\psi = \int_0^\infty \phi e^{-pt^*} dt^* \tag{A4}$$

[82] The Laplace transform of $\partial\phi_u/\partial t^*$ (respectively, $\partial\phi_c/\partial t^*$) is: $p\psi_u - \phi_0$ (respectively, $p\psi_c - \phi_0$) and the diffusion equations (A2) and (A3) become simply:

$$\frac{\partial^2 \psi_c}{\partial \xi^2} - p\psi_c = -(1+\alpha\xi)h_0 \tag{A5}$$

$$f\frac{\partial^2 \psi_u}{\partial \xi^2} - p\psi_u = -(1+\alpha\xi)h_0 \tag{A6}$$

[83] The general solutions of these differential equations are easily found as:

$$\psi_c = A_c \cosh(q_c\xi) + B_c \sinh(q_c\xi) + \frac{(1+\alpha\xi)h_0}{p} \tag{A7}$$

$$\psi_u = A_u \cosh(q_u\xi) + B_u \sinh(q_u\xi) + \frac{(1+\alpha\xi)h_0}{p} \tag{A8}$$

where q_c and q_u are defined by $q_c = \sqrt{p}$ and $q_u = \sqrt{p/f}$.

[84] The four constants A_u, B_u, A_c, B_c are computed by satisfying the previous boundary conditions:

[85] 1. at $\xi = 0, \psi_c = 0$ imposes $A_c = 0$;

[86] 2. at $\xi = 1, \partial\psi_u/\partial\xi = 0$ imposes $B_u = \alpha h_0/(pq_u)$;

[87] 3. at $\xi = \xi_c$, the conditions of potential continuity $(\psi_c = \psi_u)$ and flux continuity $(\partial\psi_c/\partial x = \partial\psi_u/\partial x)$ can be written as two linear equations for the two remaining unknowns A_u and B_c, the determinant of which is:

$$\Delta = \sqrt{f}\cosh(q_c\xi_c)\cosh(q_u\xi_u) + \sinh(q_c\xi_c)\sinh(q_u\xi_u) \tag{A9}$$

[88] The Laplace transforms ψ_c and ψ_u are easily computed as:

$$\psi_c = -\frac{\alpha h_0}{\Delta p q_u}\sinh(q_c\xi) + \frac{(1+\alpha\xi)h_0}{p} \tag{A10}$$

$$\psi_u = -\frac{\alpha h_0}{\Delta p q_u}\left[\sqrt{f}\sinh(q_u\xi_u)\cosh(q_c\xi_c) + \cosh(q_u\xi_u)\sinh(q_c\xi_c)\right] \cosh(q_u(1-\xi)) + \frac{\alpha h_0}{pq_u}\sinh(q_u(1-\xi)) + \frac{(1+\alpha\xi)h_0}{p} \tag{A11}$$

where Δ is defined above in equation (A9).

[89] The Laplace transform (LT) are now obtained. The problem is to obtain the inverse Laplace transforms (LT^{-1}).

A3. The Inverse Laplace Transform

[90] The exact LT^{-1} of equations (A10) and (A11) is based on the inversion theorem [*Carslaw and Jaeger*, 1959] which requires the evaluation of the integral of ψ along a contour in the complex p-plane:

$$\phi(t^*) = \frac{1}{2\pi i}\int_c \psi(p) e^{pt^*} dp \tag{A12}$$

[91] The contour c of the integral $\int_c$ is parallel to the imaginary axis p, running from $\gamma - i\infty$ to $\gamma + i\infty$, γ being a real value such that all singularities of the function $\psi(p)$ of the complex variable p are located in the left part of the complex p-plane. It can be verified by limited development that the function $\psi(p)$ is single valued and has no branch point associated with the dependence in q_u or q_c (it can be shown that functions such as $\sinh(q_u\xi_u)\cosh(q_c\xi_c)$, $\sinh(q_c\xi_c)/q_u$, and $\sinh((1-\xi)q_u)/q_u$ are regular). The only singularities of $\psi(p)$ are poles which make the denominator of equations (A10) and (A11) null, namely two type of poles:

[92] 1. the pole $p = 0$, called p_0

[93] 2. an infinite series of poles corresponding to the zeros of Δ, i.e., solutions of:

$$\Delta = \sqrt{f}\cosh(q_u\xi_u)\cosh(q_c\xi_c) + \sinh(q_u\xi_u)\sinh(q_c\xi_c) = 0 \tag{A13}$$

[94] The function $\Delta(p)$ becomes null when $q_c = \sqrt{p}$ is pure imaginary as, i.e., $q_c = i\beta$, (therefore, $q_u = i\beta/\sqrt{f}$). The zeros in p are then real negative or null and it can be shown [*Carslaw and Jaeger*, 1959, p. 325] that these are the only zeros of equation (A13).

[95] Hyperbolic trigonometry allows replacing equation (A13) by:

$$\Delta(\beta) = \sqrt{f}\cos\left(\frac{\xi_u\beta}{\sqrt{f}}\right)\cos(\xi_c\beta) - \sin\left(\frac{\xi_u\beta}{\sqrt{f}}\right)\sin(\xi_c\beta) = 0 \tag{A14}$$

[96] The poles in p are real: $p_0 = 0$ on the one hand and $p_n = -\beta_n^2$ on the other hand.

[97] The contour of the integral equation (A12) can be closed on a large circle in the left part of the p-plane (Real $(p) < 0$); the contribution to the integral of this latter part of the contour vanishes when the circle radius tends to ∞. Since the integral contour includes all the poles of the function ψ, the application of the theorem of residues (Cauchy's theorem) provides the final result. The LT^{-1} is written as

$$\phi(t^*) = \sum_{n=0}^{\infty} R_n e^{p_n t^*} \tag{A15}$$

where the summation $\sum$ is taken on all indices $n = 0, 1, \ldots, \infty$ of ψ poles and where the R_n are the residues of these poles (i.e., the behavior of the $\psi(p)$ in the vicinity of $p = p_n$). One obtains

[98] The potential is the sum of a constant (in fact h_0) and a series of exponential terms with negative time arguments, i.e., decreasing with reduced time t^* according to a reduced time constant β_n^{-2}. Returning to actual variables, the time constant associated with index n is:

$$\phi(t^*) = R_0 + \sum R_n e^{-\beta_n^2 t^*} \text{ for } n = 1, 2, \ldots \infty \tag{A16}$$

$$\tau_n = \frac{L^2}{D_c \beta_n^2} \tag{A17}$$

[99] The calculation of the residues $R_0, R_1, \ldots$ is straightforward:

$$R_0 = h_0 \tag{A18}$$

$$R_{nc} = 2\alpha h_0 \sqrt{f} \frac{\sin(\beta_n \xi)\sin(\beta_n \xi_u/\sqrt{f})}{\beta_n^2[1-\xi_c(1-f)\cos^2(\beta_n \xi_u/\sqrt{f})]\cos(\beta_n \xi_c)} \tag{A19}$$

$$R_{nu} = 2\alpha h_0 \, f \frac{\cos(\beta_n(1-\xi)/\sqrt{f})}{\beta_n^2[1-\xi_c(1-f)\cos^2(\beta_n \xi_u/\sqrt{f})]} \tag{A20}$$

[100] The final solution is a sum $\sum$ for $n = 1, 2, \ldots \infty$:

$$\phi_c = h_0 + 2\alpha h_0 \sqrt{f} \sum_{n=1}^{\infty} \frac{\sin(\beta_n \xi)\sin(\beta_n \xi_u/\sqrt{f})}{\beta_n^2[1-\xi_c(1-f)\cos^2(\beta_n \xi_u/\sqrt{f})]\cos(\beta_n \xi_c)} e^{-\beta_n^2 t^*} \tag{A21}$$

$$\phi_u = h_0 + 2\alpha h_0 \, f \sum_{n=1}^{\infty} \frac{\cos(\beta_n(1-\xi)/\sqrt{f})}{\beta_n^2[1-\xi_c(1-f)\cos^2(\beta_n \xi_u/\sqrt{f})]} e^{-\beta_n^2 t^*} \tag{A22}$$

[101] It may be verified that for $\xi = \xi_c$, the two expressions ϕ_c and ϕ_u and their space derivatives become identical (and therefore continuous) when taking into account equation (A13).

A4. Practical Use of the Series Development

[102] In the previous development, the time variation is ruled by the β's, the values of which require the solution of equation (A14). The only case where equation (A14) has an obvious solution is when $f = 1$; equation (A14) reduces to $\cos(\beta) = 0$ the solutions of which are $\beta_n = \pi/2 + (n-1)\pi$ for $n = 1, 2, \ldots$

[103] In the general case, β is a positive root of equation (A14). Let us call β_1 the smallest positive root of equation (A14), also written as:

$$\tan(\beta_1 \xi_c)\tan\left(\beta_1 \xi_u/\sqrt{f}\right) = \sqrt{f} \tag{A23}$$

[104] It is convenient to begin with the case where $\sqrt{f}$ is small which enables approximation of β_1. For small values of the argument β_1, the tangent function may be approached by its argument and equation (A23) is replaced by $\xi_c \xi_u \beta_1^2 \approx f$, so that

$$\beta_1 \approx \sqrt{\frac{f}{\xi_c \xi_u}} \tag{A24}$$

[105] Starting from this initial guess, the numerical solution of equation (A23) is easily obtained by Newton's tangent method. In a few iterations, the algorithm converges to the final value of β_1. The value of the next roots of equation (A14), i.e., β_n for $n = 2, 3, \ldots$ can also be computed numerically using another algorithm based on the change of sign of $\Delta(\beta)$ while increasing β. These roots are of increasing magnitude and provide decreasing contributions to the series equations (A21) and (A22) as t increases, leaving the first exponential of the series development, $\exp\left(-\beta_1^2 t^*\right)$, as the rapidly dominant term. Therefore, the first term of the series development gives a convenient approximation of the full solution.

[106] An illustration of this last statement is shown in Figure 6, using $f = 0.01$ and $\xi_c = 0.7$, which compares the result of a computation based on the full solution, either when retaining the first term (black curves), or using the first five (gray curves). As soon as $t^* > 0$, the solution when only the first term is retained is not discernible from the more complete one, which justifies the fact that only the first exponential term of the series is retained. In supporting information, it is shown that this justification holds for a wide range of values of f and ξ_c.

[107] The relaxation of the initial disturbance toward the steady state is therefore characterized by an exponential decay according to $\exp\left(-\beta_n^2 t^*\right)$, or in actual variables, $\exp(-t/\tau_m)$ with $\tau_m = L^2/\left(D_c \beta_1^2\right)$.

A5. Practical Estimate of β_1: Limits and Further Development

[108] It remains to propose a practical approximation of β_1. For low f values, the first development of $\Delta(p)$ for small p values yields a convenient approximation of the root β_1, defined by the label β_{10}:

$$\beta_{10} = \sqrt{\frac{f}{\xi_u(\xi_c + \xi_u/2)}} \tag{A25}$$

and the corresponding time constant is evaluated by:

$$\tau_{m0} = \frac{L_u}{D_u}(L_c + L_u/2) \tag{A26}$$

[109] Formula equation (A26) is interesting because of its simplicity and because it depends only on the diffusivity of the unconfined aquifer. However, it is clear that it breaks down when the length of the unconfined aquifer L_u tends to 0.

[110] More refined approximations can be obtained through a series expansion of $\Delta(\beta)$ about $\beta = 0$ through polynomial expansion of $\Delta(\beta)$ as a third degree polynomial in $\beta^2/(2f)^2$:

$$\frac{1}{\sqrt{f}}\Delta(\beta) \approx 1 - a_2\left(\frac{\beta}{2f}\right)^2 + a_4\left(\frac{\beta}{2f}\right)^4 - a_6\left(\frac{\beta}{2f}\right)^6 \tag{A27}$$

where

$$a_2 = \xi_u^2 + 2\xi_u \xi_c + f\xi_c^2 \tag{A28}$$

$$a_4 = \frac{1}{6}\left(\xi_u^4 + 4\xi_u^3 \xi_c + 6f\xi_u^2 \xi_c^2 + 4f\xi_u \xi_c^3 + f^2 \xi_c^4\right) \tag{A29}$$

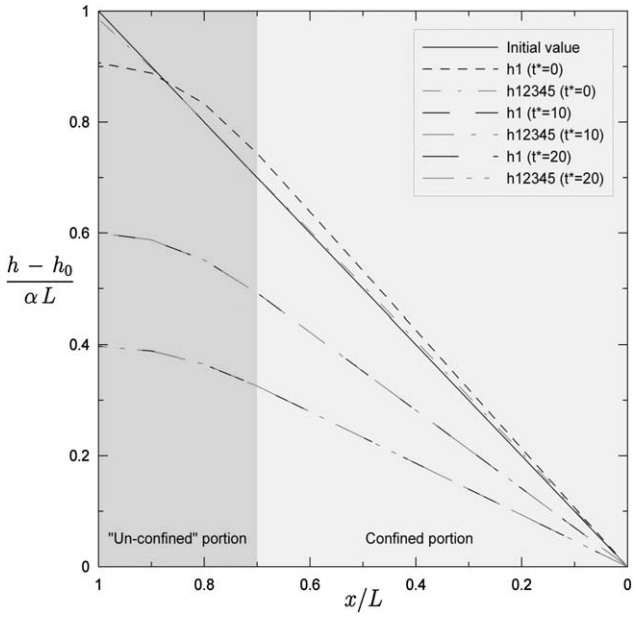

Figure 6. Reduced hydraulic potential as a function of x/L for various values of reduced time $t^* = D_c t/L^2$ (0, 10, 20). The computed time constant is $\beta_1^{-2} = 24.2$. Aquifer parameters are $f = S_u/S_c = 0.01, L_c/L = 0.7$. The computed solutions are obtained either retaining the first term (h1) or the five first ones (h12345).

$$a_6 = \frac{1}{90}\left(\xi_u^6 + 6\xi_u^5\xi_c + 15f\xi_u^4\xi_c^2 + 20\xi_u^3\xi_c^3 + 15f^2\xi_u^2\xi_c^4 + 6f^2\xi_u\xi_c^5 + f^3\xi_u^6\right) \tag{A30}$$

[111] By truncating the polynomial of equation (A27) sequentially at orders 1, 2, 3, and equating the reduced polynomials to zero, respective β_{11}, β_{12}, β_{13} approximations β_1 of the true β_1 can be found by analytical solution formulae.

[112] The estimates of β and τ_m corresponding to the first-order approximation are given by

$$\beta_{11}^2 = \frac{2f}{a_2} = \frac{2f}{\xi_u^2 + 2\xi_u\xi_c + f\xi_c^2} \tag{A31}$$

with the corresponding time constant:

$$\tau_{m1} = \frac{L_u(L_u + 2L_c)}{2D_u} + \frac{L_u^2}{2D_c} \tag{A32}$$

[113] The estimates corresponding to the second-order approximation are

$$\beta_{12}^2 = \frac{f\left[a_2 - \sqrt{a_2^2 - 4a_4}\right]}{a_4} \tag{A33}$$

$$\tau_{m2} = \frac{a_4 L^2}{D_u\left[a_2 - \sqrt{a_2^2 - 4a_4}\right]} \tag{A34}$$

[114] Contrary to equation (A25), these last estimates of β_1 are defined for any value of the unconfined aquifer length, even for $\xi_u = 0$. However, taking into account the value of f corresponding to actual situations (on the order of 10^{-3}), it is possible to compare the accuracy of these various estimates of β_1 as β_{10}, β_{11}, β_{12}, and β_{13} for a large range of the ξ_u and f parameters. This is illustrated in Table 4, where values are given for the three approximations as well as the accurate value for $f = 0.01$, 0.001, and 0.0001. The ξ_c parameter varies from 0.5 to 0.995 in order to focus on the vicinity of $\xi_u = 0$. As expected, there is an improvement in accuracy with increasing order: β_{11} is closer to β_1 than β_{10}, β_{12} is even closer, and β_{13} is the closest.

[115] The discrepancy in the vicinity of $\xi_u = 0$ is larger for the smaller values of f. However it appears that, to within about 5%, the simpler formula equation (A26) gives acceptable results for values as small as 0.05 (the unconfined aquifer then represents 5% of the total length) for $f = 0.01$; for $f = 0.001$, the approximation is correct when ξ_u is down to 0.005 and even smaller for $f = 0.0001$.

[116] Errors in the approximations of β_1 translate into errors in the series equations (A21) and (A22). These will affect not only the target value of a 95% reduction of the initial perturbation at $t = 3\tau_m$ in the exponential term $\exp\left(-\beta_1^2 t^*\right)$ but also the coefficients of this term in the two series. These coefficients cause nonlinear behavior in ϕ across the aquifer as soon as t is greater than 0, as evidenced in Figure 6. This implies that the 95% reduction, or 5% residual, relative to the initial linear perturbation cannot be uniform across the aquifer. Consequently, an averaged target value is used. Typically, the range of residuals across the aquifer is between 4% and 7% with an average just over 5% when using β_1. In supporting information, averaged residuals are calculated for a range of values of f and ξ_u for the two approximate roots β_{10} and β_{12} to determine the constraints on their usage. Setting an allowable average residual target value of 6.5% it is found that β_{10} can be used when the ratio f/ξ_u is smaller than 0.3. Returning to

Table 4. Values of β_1 and Their Approximations as a Function $L_c/L = \xi_c$ (i.e., $\xi_u = 1 - \xi_c$)[a]

ξ_c	ξ_u	β_{10}	β_{11}	β_{12}	β_{13}	β_1
$f = 0.01$						
0.5	0.5	0.163299	0.163028	0.172307	0.171905	0.171912
0.8	0.2	0.235702	0.233635	0.238779	0.238695	0.238695
0.9	0.1	0.324443	0.317741	0.322855	0.322787	0.322787
0.95	0.05	0.452911	0.433301	0.441498	0.441379	0.441379
0.98	0.02	0.710669	0.637551	0.659813	0.659253	0.659259
0.99	0.01	1.002509	0.820596	0.867007	0.865012	0.865046
0.995	0.005	1.415985	1.003133	1.086066	1.080331	1.080475
$f = 0.001$						
0.5	0.5	0.051640	0.051631	0.054527	0.054405	0.054407
0.8	0.2	0.074536	0.074469	0.075884	0.075867	0.075867
0.9	0.1	0.102598	0.102380	0.103359	0.103352	0.103352
0.95	0.05	0.143223	0.142565	0.143400	0.143396	0.143396
0.98	0.02	0.224733	0.222057	0.223319	0.223314	0.223314
0.99	0.01	0.317021	0.309492	0.312195	0.312179	0.312179
0.995	0.005	0.447774	0.427081	0.433746	0.433677	0.433678
$f = 0.0001$						
0.5	0.5	0.016330	0.016330	0.017244	0.017206	0.017207
0.8	0.2	0.023570	0.023568	0.024009	0.024003	0.024003
0.9	0.1	0.032444	0.032437	0.032726	0.032724	0.032724
0.95	0.05	0.045291	0.045270	0.045471	0.045471	0.045471
0.98	0.02	0.071067	0.070981	0.071129	0.071129	0.071129
0.99	0.01	0.100251	0.100005	0.100171	0.100171	0.100171
0.995	0.005	0.141598	0.140901	0.141191	0.141191	0.141191

[a]The results are given for three values of f: 0.01, 0.001, and 0.0001.

original physical quantities, this ratio has a specific meaning since, for ξ_u near 0, $f/\xi_u \approx S_c L_c/(S_u L_u)$. Quantity as $S_c L_c$ can be interpreted as the horizontally integrated storativity in the confined aquifer. Therefore, since f/ξ_u can be seen as the ratio of the integrated storativity of the confined aquifer to that of the unconfined one, only when the ratio is larger than 0.3, i.e., for a very small integrated storativity of the unconfined aquifer, would it be necessary to use other approximations such as β_{11} or β_{12} (which can be used for all f and ξ_u). Since the possibility that the unconfined aquifer is reduced to such a small relative length has no practical importance, it is clear that the approximation given by formula equation (A26) is relevant to the problem under study. With the range of f and ξ_u values for actual aquifers investigated in this paper formula (A26) can be used in all cases.

[117] A further question is that of initial and boundary conditions. If initial conditions are different from those used here, the effect is to change the right-hand sides of the Laplace transformed differential equations. But this will not change the determinant, Δ, given by equation (A13), and consequently the same τ_m prevails. The spatial variations of ϕ will be altered along with point wise values of percentage residuals at $t = 3\tau_m$. Although not validated, the changes in percentage residuals are expected to be slight. In *Carslaw and Jaeger* [1959, chap. 3], there are worked examples for the single type of aquifer, which show that the τ_m values are unchanged for different initial conditions. The most likely variation in end boundary conditions is to assume that at the unconfined end, gradient conditions are no longer zero, i.e., $\partial\phi/\partial x \neq 0$ at $x = L$. Again, this will not change Δ and τ_m.

[118] **Acknowledgments.** This work was funded by a grant from the Australian National Water Commission. The authors wish to thank the Editor, Harihar Rajaram, the Associate Editor, as well as S. A. Leake and a second anonymous reviewer for their comments and help on improving this paper. The authors would like to thank again S. A. Leake and two other anonymous reviewers for their constructive comments that helped to improve an initial version of this paper.

References

Alley, W. M., R. W. Healy, J. W. LaBaugh, and T. E. Reilly (2002), Flow and storage in groundwater systems, *Science*, *296*(5575), 1985–1990.

Anderson, M. P., and W. W. Woessner (1992), *Applied Groundwater Modeling. Simulation of Flow and Advective Transport*, 381 pp., Academic, San Diego, Calif.

Bear, J. (1972), *The Dynamics of Fluids in Porous Media*, 764 pp., Elsevier, New York.

Beyerle, U., R. Purtschert, W. Aeschbach-Hertig, D. M. Imboden, H. H. Loosli, R. Wieler, and R. Kipfer (1998), Climate and groundwater recharge during the last Glaciation in an ice-covered region, *Science*, *282*(5389), 731–734.

Bonotto, D. M. (2006), Hydro(radio)chemical relationships in the giant Guarani aquifer, Brazil, *J. Hydrol.*, *323*(1–4), 353–386.

Burbey, T. (2001), Stress-strain analyses for aquifer-system characterization, *Ground Water*, *39*(1), 128–136.

Burdon, D. J. (1977), Flow of fossil ground water, *Q. J. Eng. Geol.*, *10*(2), 97–124.

Carslaw, H., and J. Jaeger (1959), *Conduction of Heat in Solids*, 510 pp., Oxford Univ. Press, London.

Chen, J., C. Tang, Y. Sakura, J. Yu, and Y. Fukushima (2004), Nitrate pollution from agriculture in different hydrogeological zones of the regional groundwater flow system in the North China Plain, *Hydrogeol. J.*, *13*, 481–492, doi:10.1007/s10040-004-0321-9.

Chiang, W.-H., and W. Kinzelbach (1998), Processing Modflow: A Simulation System for Modeling Groundwater Flow and Pollution. [Available at http://www.iwhw.boku.ac.at/hydsem2/pmwin5.pdf.].

Coudrain, A., A. Talbi, E. Ledoux, M. Loubet, J. Vacher, and E. Ramirez (2001), Subsurface transfer of chloride after a lake retreat in the Central Andes, *Ground Water*, *39*(5), 751–759.

Cramer, B., H. Poelchau, P. Gerling, N. Lopatin, and R. Littke (1999), Methane released from groundwater: The source of natural gas accumulations in northern West Siberia, *Mar. Pet. Geol.*, *16*(3), 225–244.

Custodio, E. (2002), Aquifer overexploitation: What does it mean?, *Hydrogeol. J.*, *10*(2), 254–277.

de Marsily, G. (1986), *Quantitative Hydrogeology: Groundwater Hydrology for Engineers*, 440 pp., Academic, San Diego, Calif.

de Vries, J. (1997), Prediction in hydrogeology: Two case histories, *Geol. Rundsch.*, *86*(2), 354–371.

Dieng, B., E. Ledoux, and G. De Marsily (1990), Palaeohydrogeology of the Senegal sedimentary basin: A tentative explanation of the piezometric depressions, *J. Hydrol.*, *118*(1–4), 357–371.

Domenico, P. A., and F. W. Schwartz (1998), *Physical and Chemical Hydrogeology*, 2nd ed., 506 pp., John Wiley, New York.

Douez, O. (2007), Réponses d'un système aquifère multicouche aux variations paléoclimatiques et aux sollicitations anthropiques—Approche par modélisation couplée hydrodynamique, thermique and géochimique, PhD thesis, Univ. Bordeaux 3.

Gonçalvès, J., S. Violette, and J. Wendling (2004), Analytical and numerous solutions for alternative overpressuring preocesses: Application to the Callovo-Oxfordian sedimentary sequence in the Paris basin, France, *J. Geophys. Res.*, *109*, B02110, doi:10.1029/2002JB002278.

Habermehl, M. A. (1980), The Great Artesian Basin, Australia, *BMR J. Aust. Geol. Geophys.*, *5*(1), 9–38.

Han, Z. (2008), Alluvial aquifers in the North China plain, in *Aquifer Systems Management: Darcy's Legacy in a World of Impending Water Shortage*, edited by L. Chery and G. de Marsily, pp. 117–126, Taylor and Francis, London.

Harbaugh, A. W., and M. G. McDonald (1996), User's documentation for MODFLOW-96, an update to the U.S. Geological Survey modular finite-difference ground-water flow model, *Open File Rep. 96-485*, U.S. Geol. Surv., Reston, Va.

Heathcote, J. A., and U. M. Michie (2004), Estimating hydrogeological conditions over the last 120 ka: An example from the Sellafield area, UK, *J. Geol. Soc.*, *161*(6), 995–1008.

Houston, J., and D. Hart (2004), Theoretical head decay in closed basin aquifers: An insight into fossil groundwater and recharge events in the Andes of northern Chile, *Q. J. Eng. Geol. Hydrogeol.*, *37*(2), 131–139.

Imbrie, J., et al. (1992), On the structure and origin of major galaciation cycles, 1. Linear responses to Milankovitch forcing, *Paleoceanography*, *7*(15), 701–738.

Jost, A. (2005), Caractérisation des forçages climatiques et géomorphologiques des cinq derniers millions d'années et modélisation de leurs conséquences sur un système aquifère complexe: le bassin de Paris, PhD thesis, Univ. Pierre et Marie Currie.

Jost, A., S. Violette, J. Gonçalvès, E. Ledoux, Y. Guyomard, F. Guillocheau, M. Kageyama, G. Ramstein, and J.-P. Suc (2007), Long-term hydrodynamic response induced by past climatic and geomorphologic forcing: The case of the Paris basin, France, *Phys. Chem. Earth*, *32*(1–7), 368–378.

Keppel, M., K. E. Karlstrom, A. J. Love, S. Priestley, D. Wohling, and S. De Ritter (2013), Allocating water and maintaining springs in the Great Artesian Basin, in *Volume I: Hydrogeological Framework of the Western Great Artesian Basin*, Natl. Water Comm., Canberra, Australia.

Kershaw, A. P., and G. C. Nanson (1993), The last full glacial cycle in the Australian region, *Global Planet. Change*, *7*(1–3), 1–9.

Kimmelmann e Silva, A. A., A. C. Rebouças, and M. F. Santiago (1989), 14C analyses of groundwater from the Botucatu aquifer system in Brazil, *Radiocarbon*, *31*(3), 926–933.

Leake, S. (1990), Interbed storage changes and compaction in models of regional groundwater flow, *Water Resour. Res.*, *26*(9), 1939–1950.

Lloyd, J. W., and M. H. Farag (1978), Fossil ground-water gradients in arid regional sedimentary basins, *Ground Water*, *16*(6), 388–393.

Love, A. J., A. L. Herczeg, F. W. Leaney, M. F. Stadter, J. C. Dighton, and D. Armstrong (1994), Groundwater residence time and palaeohydrology in the Otway Basin, South Australia: ^{2}H, ^{18}O and ^{14}C data, *J. Hydrol.*, *153*(1), 157–187, doi:10.1016/0022-1694(94)90190-2.

Love, A. J., P. Shand, L. Crossey, G. Harrington, and P. Rousseau-Gueutin (2013a), *Allocating Water and Maintaining Springs in the Great Artesian*

Basin, Volume III: Groundwater Discharge of the Western Great Artesian Basin, Natl. Water Comm., Canberra.

Love, A. J., D. Wohling, S. Fulton, P. Rousseau-Gueutin, and S. De Ritter (2013b), Allocating water and maintaining springs in the Great Artesian Basin, in *Volume II: Groundwater Recharge, Hydrodynamics and Hydrochemistry of the Western Great Artesian Basin*, edited by M. Keppel et al., Natl. Water Comm., Canberra, Australia.

Luo, X. (1994), Modélisation des surpressions dans les bassins sédimentaires et des phénomènes associés, PhD thesis, Univ. Montpellier 2.

Marty, B., T. Torgessen, V. Meynier, R. K. O'Nions, and G. de Marsily (1993), Helium isotope fluxes and groundwater ages in the Dogger Aquifer, Paris Basin, *Water Resour. Res.*, *29*(4), 1025–1035.

McDonald, M. G., and A. W. Harbaugh (1988), MODFLOW, A modular three-dimensional finite difference ground-water flow model, *Open File Rep. 83-875*, U.S. Geol. Surv., Washington, D. C.

Naish, T. R., et al. (1998), Astronomical calibration of a southern hemisphere plio-pleistocene reference section, Wanganui Basin, New Zealand, *Quat. Sci. Rev.*, *17*(8), 695–710.

Nativ, R., and D. Smith (1987), Hydrogeology and geochemistry of the Ogallala Aquifer, Southern High Plains, *J. Hydrol.*, *91*(3), 217–253.

Neuzil, C. E. (1986), Groundwater flow in low-permeability environments, *Water Resour. Res.*, *22*(8), 1163–1195, doi:10.1029/WR022i008p01163.

Neuzil, C. E. (1995), Abnormal pressures as hydrodynamic phenomena, *Am. J. Sci.*, *295*(6), 742–786.

Palciauskas, V. V., and P. Domenico (1989), Fluid pressures in deforming porous rocks, *Water Resour. Res.*, *25*(2), 203–213.

Reilly, T. E., and A. W. Harbaugh (2004), Guidelines for evaluating ground-water flow models, *U.S. Geol. Surv. Sci. Invest. Rep. 2004-5038*, Reston, Va.

Riley, F. S. (1969), Analysis of borehole extensometer data from central California, in *Land Subsidence, Publ. 89, vol. 2, Proceedings of the Tokyo Symposium, 1969*, edited by L. Tyson, pp. 423–431, IASH/AIHS-UNESCO.

Schwartz, F. W., E. A. Sudicky, R. G. McLaren, Y.-J. Park, M. Huber, and M. Apted (2009), Ambiguous hydraulic heads and 14C activities in transient regional flow, *Ground Water*, *48*(3), 366–379, doi:10.1111/j.1745–6584.2009.00655.x.

Sefelnasr, A. M. (2007), Development of groundwater flow model for water resources management in the development areas of the western desert, Egypt, PhD thesis, Martin Luther Univ., Halle-Wittenberg.

Stone, H. L. (1968), Iterative solution of implicit approximations of multidimensional partial differential equations, *SIAM J. Numer. Anal.*, *5*(3), 530–558.

Sy, M. O. B., and M. Besbes (2008), Holocene and present recharge of the Saharan aquifers: A numerical modelling study, in *Aquifer Systems Management: Darcy's Legacy in a World of Impending Water Shortage*, edited by L. Chery and G. de Marsily, pp. 191–205, Taylor and Francis, London.

Tiedemann, R., M. Sarnthein, and N. J. Shackleton (1994), Astronomic timescale for the Pliocene Atlantic $\delta^{18}O$ and dust flux records of Ocean Drilling Program site 659, *Paleoceanography*, *9*(4), 619–638.

Tóth, J., and I. Almàsi (2001), Interpretation of observed fluid potential patterns in a deep sedimentary basin under tectonic compression: Hungarian Great Plain, *Pannonian Basin, Geofluids*, *1*(1), 11–36.

Urbano, L. D., M. Person, K. Kelts, and J. S. Hanor (2004), Transient groundwater impacts on the development of paleoclimatic lake records in semi-arid environments, *Geofluids*, *4*(3), 187–196.

Welsh, W. D. (2007), Groundwater balance modelling with Darcy's law, PhD thesis, The Australian National Univ.

York, J. P., M. Person, W. J. Gutowski, and T. C. Winter (2002), Putting aquifers into atmospheric simulation models: an example from the Mill Creek Watershed, northeastern Kansas, *Adv. Water Resour.*, *25*, 221–238.